
Empirical expressions for gas hydrate stability law, its volume fraction and mass-density at temperatures 273.15 K to 290.15 K

Zhengquan Lu^{1, 2, *} and Nabil Sultan¹

¹ Département de Géosciences Marines, IFREMER Centre de Brest, Plouzané Cedex 29280, France

² Institute of Mineral Resources, Chinese Academy of Geological Sciences, Beijing 100037, P.R. China

*: Corresponding author : Zhengquan Lu, email address : luzhq@vip.sina.com

Abstract:

A series of empirical expressions for predicting gas hydrate stability, its volume fraction out of pore space and gas hydrate mass-density were established in different systems in consideration of gas composition (CH₄, C₂H₆, H₂S) and salinity (NaCl, seawater), and pore size at temperature between 273.15 and 300 K, based on our gas hydrate thermodynamic model (Sultan *et al.*, 2004b, c). Six of the developed expressions for predicting gas hydrate stability were validated against the available published experimental data and they were also compared with other models. At temperature 273.15 to 290.15 K, the ARDPs (Average Relative Deviation of Pressures between the prediction and the experimental data) have shown that these empirical expressions are in agreement with the experimental data as well as other models, indicating their reliability of predicting gas hydrate stability for these systems. At higher temperatures, the empirical predictions for gas hydrate stability do not well reproduce the experimental data, because they are based on van der Waals model. The empirical expressions for predicting gas hydrate stability in the systems of CH₄ + H₂S + H₂O, CH₄ + seawater + poresize, CH₄ + H₂S + NaCl and CH₄ + CO₂ + NaCl, and for evaluating gas hydrate fraction and its density need further validation due to lack of available published experimental data. However, the empirical expressions for gas hydrate fraction and its density show that the effects of pore size and salinity are negligible; gas hydrate fraction will increase if methane concentration continuously increases relatively in excess of methane solubility and decreases with pressure within gas hydrate stability zone, which is well consistent with data of natural gas hydrates in Cascadia; gas hydrate density tends to increase with ethane percentage and decrease with pressure.

Keywords: gas hydrate, stability law, fraction out of pore space, mass-density, empirical expressions

1. Introduction

Gas hydrates are becoming more and more attractive not only because of their world-wide occurrences (Charlou et al., 2004) with a great amount of potential energy (Kvenvolden, 1995; Milkov, 2004), but also because of their great effects: blocking oil and gas pipelines (Hammerschmidt, 1934), causing the marginal continental slope instabilities (Dillon et al., 2001; Maslin et al., 2005; Sultan et al., 2004a), affecting the carbon flux balance and leading to the global warming (Dickens, 2001; Kvenvolden, 2002). Gas hydrate appears as ice-like solid clathrate formed by host lattices of water molecules that embrace small guest molecules (such as methane) stabilizing the cavities (Sloan, 1998). Among the relevant issues on gas hydrates, their formation conditions, their fraction out of pore space and the density are perhaps the three most interesting fundamental aspects to earth scientists. In recent years, numerous theoretical models are proposed about the gas hydrate stability (Handa, 1990; Bakker et al., 1996; Rempel and Buffett, 1997, 1998; Zatsepina and Buffet, 1997, 1998; Sloan, 1998; Xu and Ruppel, 1999; Henry et al., 1999; Clennell et al., 1999; Davie and Buffett, 2001; Klauda and Sandler, 2003; Sultan et al., 2004b, 2004c; Zhang et al., 2005). Most of them are derived from the van der Waals's thermodynamic theory (van der Waals and Platteeuw, 1959) with the relevant calculated or experimental parameters. Whereas some of them do not consider the dynamic factors affecting gas hydrate occurrences such as the balance of the supply and the diffusion of gases, the salinity and the effect of pore size in marine environments, Rempel and Buffett (1998) and Xu and Ruppel (1999) solve the models of gas hydrate stability and occurrence in the view of the gas advection-diffusion system. Zatssepina and Buffet (1998) and Davie and Buffett (2001) simulate the gas hydrate formation in terms of both the salinity and the methane flux in consideration of gas diffusion. Capillary effects on gas hydrate formations are also taken into consideration (Clennell et al., 1999; Henry et al., 1999; Klauda and Sandler., 2003). On the other hand, many empirical expressions for gas hydrate formations are also given (Cisternas and Lam, 1991; Elgibaly and Elkamel, 1998; Østergaard et al., 2000, 2005; Masoudi and Tohidi, 2005; Tishchenko et al., 2005). These empirical models put emphasis on inhibitors and salts affecting gas hydrate formations. However, there are few theoretical or empirical models concerned with the gas hydrate fraction out of pore space and the density.

In this work, based on our gas hydrate thermodynamic model (Sultan et al., 2004b, 2004c), empirical expressions for gas hydrate formation, its fraction and gas hydrate density are established for different systems in consideration of gas composition, and/or salinity, and/or pore size. Afterwards, the predicted results are compared with the available published experimental data on gas hydrate stability. These expressions aim at providing an empirical solution for gas hydrate quick predictions. And the empirical expression for predicting gas hydrate density may also be used to evaluate the continental slope instability. Actually gas hydrate dissociation is an important factor affecting the seafloor morphology (Sultan et al., 2004c), and meanwhile it inevitably changes the gas hydrate-bearing layer's density.

2. Theoretical bases for gas hydrate characterization and quantification

The following key equation is used to cope with the two-phase chemical potential equilibrium relation involving gas hydrate characterization:

$$\Delta\mu^0 + RT \int_{P_0}^P \frac{\Delta V_w}{RT} dp - RT \int_{T_0}^T \frac{\Delta H_w}{RT^2} dT - RT \ln(\gamma_w X_w) + RT \sum_{j=1}^2 \nu_j \ln\left(1 - \sum_i^n y_{ij}\right) = \frac{2\sigma V_h}{r_p} \cos \theta \quad (1)$$

On the left side the first four terms represent the difference of the chemical potential of water between the empty hydrate lattice and the liquid phase, and the last fifth is the difference of the chemical potential of water between the hydrate phase and the empty hydrate lattice (Van der Waals and Platteeuw model, 1959; Sloan, 1998); the right-hand term corresponds to the capillary effect on the hydrate phase equilibrium (Henry et al., 1999); $\Delta\mu^0$, ΔV_w , ΔH_w are the water chemical potential difference at the reference condition ($T_0 = 273.15K$, $P_0 = 0.101328MPa$), the water molar volume difference, the water enthalpy difference between the empty hydrate lattice and the liquid phase respectively; R is the ideal gas constant; T and P are the hydrate equilibrium temperature and

pressure; X_w , γ_w are the water mole fraction and its activity coefficient; j denotes the cavity type which guest molecules can occupy, v_j is the number of type j cavities per water molecule in the lattice, and y_{ij} is the fractional occupancy of type j cavity taken by guest molecule i , which can be further calculated in relation to the gas fugacity and the Langmuir constant; σ is the interfacial energy of the hydrate-water interface; θ is the hydrate-water contact angle; r_p is the pore radius; and V_h is the water molar volume in the hydrate lattice.

It is clear that the water salinity has an effect on the hydrate equilibrium conditions. Its effect is computed according to the Dickens and Quinby-Hunt (1997) approach. The capillary effect may reduce the hydrate equilibrium temperature by about two degrees at given pressure (Henry et al., 1999).

The hydrate fraction depends on the gas supply, its solubility and the gas to water ratio in the hydrate phase. For a given gas concentration G_i in a pore water system, the volume hydrate fraction η can be calculated in the following equation (e.g. $G_i > x_i$, where x_i is the gas i solubility at the hydrate equilibrium pressure and its computation method is given in Handa (1990)):

$$\eta = \frac{\sum_i (G_i - x_i) n_i V_h}{\sum_i (G_i - x_i) n_i V_h + (1 - \sum_i (G_i - x_i) n_i) V_l + \sum_i x_i V_i} \quad (2)$$

where $1/n_i$ ($n_i = \frac{1}{\sum_j v_j y_{ij}}$) is the gas i to water ratio in the hydrate phase; V_l is the partial

molar volume of H₂O in the aqueous solution, and V_i , the partial molar volume of gas component i in the vapour.

The mass density φ_H of hydrate can then be expressed by:

$$\varphi_H = \frac{M_{H_2O} + \sum_i \frac{M_i \sum_i n_i}{n_i}}{V_h} \quad (3)$$

where M_{H_2O} is the water molar mass and M_i is the gas i molar mass.

3. Empirical expressions of gas hydrate stability and their validation

The general procedure of this work can be divided into four steps: 1) designing appropriate systems; 2) producing a series of data by running our gas hydrate thermodynamic model (Sultan et al., 2004b, 2004c) for the use of the next step; (3) constructing appropriate empirical expressions to best characterize our model-produced data of the second step (Sultan et al., 2004b, 2004c); (4) validating the empirical expressions possibly against predecessors' published experimental data and other models.

In the course of empirically modelling, the designed systems are listed in Table 1. For each system, originally, the temperature changes from 273.15K to 300K and pressure ranges from 1.5×10^6 Pa to 4.0×10^7 Pa (150m to 4000m water depth) so as to get a broader view of our model-produced data (Sultan et al., 2004b, 2004c). All the gas compositions and salinity are given by units of mol gas per mol water, mol ion per mol water respectively.

3.1. System of pure methane and water

In the case of pure methane and pure water, after correlating our gas hydrate thermodynamic modelled-produced data (Sultan et al., 2004b, 2004c), gas hydrate (structure-I) stability can be best expressed as:

$$P(T) = \exp(AT)B \quad (4)$$

where P is pressure (kPa) and T is temperature (K), A and B are coefficients with ten digitals (Table 2). This empirical expression is compared with some of predecessors' published experimental data as well as with other available models. The compared errors in terms of RDP and ARDP are listed in Table 3 (RDP is the relative deviation of pressures between the prediction and the published

experiment data, in percents, $RDP = \frac{|P_{prediction} - P_{data}|}{P_{data}} \times 100\%$, and ARDP is the average RDP,

$$ARDP = \frac{\sum RDP}{n}.$$

The ARDPs are 2.08%, 1.49%, 2.24%, 1.47% and 1.52% with respect to the published experimental data (Table 3). Generally the ARDPs of smaller than 5% are considered as acceptable. It shows that the predicted gas hydrate formation conditions from the empirical expression for pure methane and pure water system are well consistent with the experimental measurements. The predicted results are also generally in agreement with other models (Sultan et al., 2004b; Sloan, 1998; Handa, 1990), especially at low temperatures below 290K (Fig. 1).

3.2. System of methane and ethane with pure water

Although gas hydrates are possibly transformed from structure-I to structure-II under certain conditions in pure water system (Subramanian et al., 2000), they are still considered as Structure-I in this paper. Considering the fact that in natural submarine environments, methane contents are usually greater than 90%, thus in this system only the case with ethane percentage lower than 10% is considered and the empirical expression can be given as:

$$P(T) = \exp((Ce.Me + De).T) \exp(Ee.Me).Fe \quad (5)$$

where Me is mol percentage of ethane with respect to methane ($0 < Me \leq 10$); coefficients Ce , De , Ee , Fe are given with ten digitals in Table 2.

For the mixture of methane and ethane with pure water system, the ARDPs reach 1.23%, 2.74% and 7.18% with the cases of 1.1, 2.1 and 4.8 ethane percentages of the mixture respectively (Table 3), showing that the predicted results agree well with the experimental data (Fig. 2) and that the empirical expression works better at lower ethane percentage. As the gas hydrate equilibrium pressure does not decrease strictly proportionally with the increase of ethane percentage in this case due to gas hydrate structure changes (Maekawa, 2001), the relatively growing difference between the prediction and the experimental data with the increase of ethane percentage is explainable. Additionally the comparisons with other models also indicate that they differ little within the given temperature range, especially below the temperature of 285K.

3.3. System of methane and hydrogen sulphide with pure water

In marine sediments hydrogen sulphide contents are generally supposed to be low (e.g. 2.5% H_2S +97.5% CH_4 , Shipboard Scientific Party, 2003). Therefore, for this system the case of hydrogen sulphide concentration with respect to methane lower than 3% is just considered. The correlated expression of gas hydrate (structure-I) stability to hydrogen sulphide percentage can be written as:

$$P(T) = \exp((Ch.Mh + Dh).T) \exp(Eh.Mh).Fh \quad (6)$$

where Mh is mol hydrogen sulphide percentage with respect to methane ($0 < Mh \leq 3$); coefficients Ch , Dh , Eh , Fh are presented with ten digitals in Table 2.

3.4. System of methane and carbon dioxide with pure water

It was reported by Servio et al. (1999) that gas hydrates formed from the mixture of 20 vol% CO_2 and 80 vol% CH_4 in pure water are structure-II. However, Takeya et al. (2006) found that gas hydrates encasing 96%-98% methane and a small amount of CO_2 are type-I in the submarine environment of Okhotsk sea. In this work gas hydrates formed from the mixture of methane and CO_2 are assumed as structure-I. Hence the best curve for this system can be expressed as:

$$P(T) = \exp((Cc.Mc + Dc).T) \exp(Ec.Mc).Fc \quad (7)$$

where Mc is mol carbon dioxide percentage with respect to methane ($0 < Mc \leq 20$), and coefficients Cc, Dc, Ec, Fc are presented with ten digitals in Table 2.

For the system of pure water with the mixture of methane and carbon dioxide, the comparisons are only conducted between the predicted results and the experimental data with 80mol% methane and 20mol% CO_2 (Table 3, Fig. 3) based on available references (Dholabhai et al., 1994; 1997; Servio et al., 1999; Seo et al., 2001). The ARDPs between the predicted results and the experimental data are calculated to be 12.36%, 8.14% and 10.53% with respect to data of Dholabhai et al. (1994, 1997), Servio et al. (1999) and Seo et al. (2001) respectively. The big differences are probably related to the relative high content of CO_2 in relation to methane. However, at lower temperatures, the differences between them seem smaller than they are at higher temperatures. When compared with other models, our predicted results are intermediate between models of Sultan et al. (2004b) and Sloan (1998), suggesting a general agreement between them.

3.5. System of salt water with pure methane

Experimental data indicate that Cl^- plays a predominant role in affecting gas hydrate stability in pore water (Lu et al., 2005) compared with other anions (such as SO_4^{2-} , PO_4^{3-} , CO_3^{2-}) and cations (such as Na^+ , K^+ , Ca^{2+} , Mg^{2+} , NH_4^+). In this paper, the content of NaCl out of pore water is just taken as the salinity affecting gas hydrate (structure-I_s) stability.

To better get the correlation, the salinity up to 0.050 mol NaCl / mol H_2O (13.966wt% NaCl) is taken into consideration, about four times as much as seawater. The empirical expression can be expressed as:

$$P(T, S) = \exp((Cs.S + Ds).T) \exp(Es.S).Fs \quad (8)$$

where S is salinity in pore water ($0 < S \leq 0.050 \text{ mol NaCl / mol } H_2O$), and coefficients Cs, Ds, Es, Fs are given with ten digitals in Table 2.

For the pure methane and various pore water systems, the compared results are listed in Table 3: when the salinity is 3.0wt%NaCl, the difference between the predicted results and the experimental data of Maekawa (2001), the ARDP, is 3.61%; when the salinity is 3.35wt% NaCl, the ARDP is 4.91% between the predicted results and the experimental data of Dickens et al. (1994); and when the salinity is 0.02001 mol NaCl per mol pore water, the ARDP is 8.47% between the predicted results and the experimental data of Jager et al. (2001). These results show that with the increase of salinity the ARDPs gradually increase. When compared with other models (Sultan et al., 2004b; Sloan, 1998), it can still be seen that they are in agreement with them within the given temperature range (Fig. 4).

3.6. System of pure water / seawater with various pore sizes

When the predicted gas hydrate stability zone does not coincide with the real submarine gas hydrate occurrence, the theory of pore capillary is well applied to explain the difference (Clennell et al., 1999; Henry et al., 1999). To analyse gas hydrate stability dependence on the pore size, the case of pure methane and pure water is first given. The pore size changes from $6 \times 10^{-9} \text{ m}$ to $1 \times 10^{-6} \text{ m}$ of the pore radius. Actually, this pore size range generally covers the span of marine sediment pore size (the average is around $1 \times 10^{-7} \text{ m}$, Griffiths et al., 1989; Henry et al., 1999). And this designed pore size range also embraces the ever-proposed pore radius range (550-600Å) of sensibility to gas hydrate equilibrium (Turner et al., 2005). In this system, gas hydrate (structure-I_s) stability curve can be correlated as:

$$P(T) = \exp\left(\left(Ra \cdot \frac{1}{r_p} + Rb\right)T\right) \cdot \left(Rc \cdot \frac{1}{r_p} + Rd\right) \quad (9)$$

where r_p is the pore radius (from 6×10^{-9} to $1 \times 10^{-6} \text{ m}$), and coefficients of parameters Ra, Rb, Rc, Rd are listed with ten digitals in Table 2.

Similarly, for the system of pure methane and seawater, the empirical gas hydrate (structure-I_s) stability curve can still be expressed as Equations (9), but with different coefficient values (Table 2).

For the system of pure methane and pure water with different pore sizes, scientists (Handa, 1992; Uchida et al., 1999, 2002; Anderson et al., 2003) carried out comparatively a large quantity of relevant experiments about the effect of different pore sizes on gas hydrate formation, which make it possible to compare the predicted results with the experimental data in a broad extent of pore sizes (Table 3, Fig. 5). Through calculations, it is seen that when the pore sizes are 7.0nm, 9.2nm, 10.nm, 15.8nm,

30.0nm, 30.6nm, 50.0nm and 100 nm, the ARDPs are 6.20%, 11.57%, 12.54%, 4.35%, 2.68%, 2.64%, 2.08%, and 2.64% respectively. When the pore size is 6.0nm, the ARDP reaches 22.83%, but these two sets of experimental data (Uchida et al., 2002) are obviously deflecting away from others (Fig. 5), even compared with the similar pore size (7.0nm) experimental data (Handa and Stupin, 1992), possibly indicating some experimental errors. However, the differences between the predicted results and the experimental data generally decrease with the increase of pore size, suggesting that the empirical expression works better with the increase of the mean pore size. Except the cases with pore sizes of 9.2nm and 10.0nm, the ARDPs are lower than 6.20%, showing good agreements between the predicted results and the experimental data. Especially when pore sizes are greater than 10.0nm, all the ARDPs are lower than 4.35%, indicating that the empirical expression works well with the pore size greater than 10.0nm, and this pore size is one magnitude lower than the expected mean pore size in natural environments (1×10^{-7} m, Griffiths et al., 1989; Henry et al., 1999).

3.7. System of salt water with different gas mixtures

Based on the work for systems of pure water with the mixture of methane and ethane, pure water with the mixture of methane and hydrogen sulphide, and pure water with the mixture of methane and carbon dioxide, the empirical expressions for gas hydrate (structure-I)s stability in systems of salt water with gas mixture of methane and ethane, salt water with gas mixture of methane and hydrogen sulphide, and salt water with gas mixture of methane and carbon dioxide can be further correlated to salinity respectively (Equation (10), (11), (12)):

$$P(T) = \exp(((Ce_1.S + Ce_2).Me + De_1.S + De_2).T) \cdot \exp((Ee_1.S + Ee_2).Me) \cdot (\exp(Fe_1.S) + Fe_2) \quad (10)$$

where S is the salinity ($0 < S \leq 0.08014 \text{ molNaCl} / \text{molH}_2\text{O}$); Me is the ethane percentage ($0 < Me \leq 5$); $Ce_1, Ce_2, De_1, De_2, Ee_1, Ee_2, Fe_1, Fe_2$ are presented with ten digitals in Table 2.

$$P(T) = \exp(((Ch_1.S + Ch_2).Mh + Dh_1.S + Dh_2).T) \cdot \exp((Eh_1.S + Eh_2).Mh) \cdot (\exp(Fh_1.S) + Fh_2) \quad (11)$$

where S is the salinity ranging ($0 < S \leq 0.05994 \text{ molNaCl} / \text{molH}_2\text{O}$); Mh is the H_2S percentage ($0 < Mh \leq 3$); $Ch_1, Ch_2, Dh_1, Dh_2, Eh_1, Eh_2, Fh_1, Fh_2$ are enumerated with ten digitals in Table 2.

$$P(T) = \exp(((Cc_1 + Cc_2.S + Cc_3.S^2).Mc + Dc_1.S + Dc_2).T) \cdot ((Ec_1 + Ec_2.S + Ec_3.S^2).Mc + \exp(Fc_1.S) \cdot Fc_2) \quad (12)$$

where S is the salinity ($0 < S \leq 0.05994 \text{ molNaCl} / \text{molH}_2\text{O}$); Mc is the CO_2 percentage ($0 < Mc \leq 3$); $Cc_1, Cc_2, Cc_3, Dc_1, Dc_2, Ec_1, Ec_2, Ec_3, Fc_1, Fc_2$ are listed with ten digitals in Table 2.

In the system of pore water with the mixture of methane and ethane, only one example is given with salinity of 3.0 wt% NaCl out of pore water based on the experimental data of Maekawa (2001). When ethane percentage is 2.1 in the mixture, the ARDP is calculated to be 5.68% and when ethane percentage is 4.8 in the mixture, the ARDP is 11.56% (Table 3). The compared results show that the errors between the predictions and the experimental data grow with the increase of ethane percentage (Fig. 6), suggesting that the predicted expression works better at lower ethane percentage in this system. At high ethane percentage of the mixture in pore water, the increasing difference between the prediction and the experimental data is probably caused by gas hydrate structure transformation, which is reported by experimental results (Maekawa, 2001). When compared with other models (Sultan et al., 2004b; Sloan, 1998), it is shown that the differences between the predicted results and the models are not big.

It should be pointed out that among all the empirical expressions some can not be validated due to lack of experimental data and thus need to be further confirmed. However, as all the empirical expressions proposed in this paper are just intended for structure-I gas hydrate equilibrium predictions, it is not yet known whether some ARDPs with more than 5% are partially caused by the discrepancy between the predicted and the experimental gas hydrate structures or by other reasons.

Furthermore, in principle $De, Dh, Dc, Ds, De_2, Dh_2, Dc_2, Rb$ are equal to A , and $Fe = Fh = Fc = Fs = Fe_2 = Fh_2 = Fc_2 = Rd = B$, $Ce_2 = Cc$, $Ee_2 = Ee$, $Ch_2 = Ch$, $Eh_2 = Eh$, $Cc_1 = Cc$, but the empirical expressions for different systems are deduced individually, inevitably leading to the coefficient differences. However, these small coefficient differences for various equations with the same given initials, as a matter of fact, cause little temperature offset on the average with respect to the system of pure water and pure methane (e.g. 0.03K, 0.07K, 0.17K, 0.43K), indicating that the separate expressions do not affect the predictions much for the interconnected systems.

4. Empirical expressions of gas hydrate fraction, its density and their discussions

4.1. Empirical expression of gas hydrate fraction

It is very complex to propose a unified empirical expression for gas hydrate fraction considering all the factors such as temperature or pressure, gas composition, salinity and pore size. The differences of gas hydrate fractions resulted from different pore sizes and from different salinities are very small, suggesting that the pore size and the salinity have practically little influence on the gas hydrate fraction.

Hence in this paper in the course of deducing the empirical expression for gas hydrate fraction, the case of pure methane and pure water is only taken into consideration. With the similar procedures to the previous part, for this system the empirical expression can be best fitted as:

$$Fr(P, M) = (Fa_1 \cdot \exp(Fa_2 \cdot M) + Fa_3 \cdot M^{Fa_4}) \cdot \ln(P) + Fb_1 \cdot \exp(Fb_2 \cdot M) + Fb_3 \cdot M^{Fb_4} \quad (13)$$

where Fr is the gas hydrate fraction; P stands for pressure (kPa); M is methane concentration (0.004 to 0.15 mol / mol H₂O); coefficients $Fa_1, Fa_2, Fa_3, Fa_4, Fb_1, Fb_2, Fb_3, Fb_4$ are given with ten digitals in Table 4.

4.2. Empirical expression of gas hydrate density

Preliminary calculations have shown that pore sizes, salinity and pure methane system have practically little influence on the density of the gas hydrate layer. Thus in this paper the case of mixture of methane and ethane in pure water system is only considered. The empirical expression of gas hydrate mass-density can then be expressed as:

$$Ds(P, Me) = (Da_1 + Da_2 \cdot Me + Da_3 \cdot Me^2) \cdot \exp((Db_1 \cdot \ln(Me) + Db_2) \cdot P) + \exp(Dc_1 \cdot Me) \cdot Dc_2 \cdot P^{Dd_1 + Dd_2 \cdot Me + Dd_3 \cdot Me^2} \quad (14)$$

where Ds is the density (g/cm³); P is the pressure; Me is the ethane percentage in the mixture ($1 \leq Me \leq 3$); $Da_1, Da_2, Da_3, Db_1, Db_2, Dc_1, Dc_2, Dd_1, Dd_2, Dd_3$ are listed with ten digitals in Table 4.

4.3. Discussions on gas hydrate fraction and gas hydrate density

Due to lack of experimental data on gas hydrate fraction and gas hydrate density, the empirical expressions for the gas hydrate fraction and the gas hydrate density cannot be validated at the moment. However, from Equation (2) and (3) it can be seen that the two major parameters controlling gas hydrate fraction values are the gas solubility and the ratio of gas to water in the hydrate phase. Deaton and Frost (1946) experimentally measured the gas to water ratio for several gas hydrate systems. At the temperature 273K, they showed the methane to water ratio in the hydrate phase was about 142 or 143 mmol CH₄/mol H₂O. Lorenson and Collett (2000) reported that the gas to water ratio is comprised of 121 to 173 mmol CH₄/mol H₂O depending on the temperature and pressure conditions. Results from Deaton and Frost (1946) and from Lorenson and Collett (2000) fit well with the Sultan et al. (2004b) predictions (155 mmol CH₄/mol H₂O at around 273.5K and 162 mmol CH₄/mol H₂O at around 282 K).

The solubility of methane in water rises with the increase of P or falls with the increase of T before gas hydrates are formed and during gas hydrate crystallization the solubility keeps constant (Handa, 1990; Sultan et al., 2004b; Davie et al., 2004), and thus the gas hydrate fraction will grow with the duration of gas hydrate crystallization if methane is continuously provided in excess to the solubility. For different gas hydrate equilibria, the gas solubility in water rises with P or T increase. In marine environments, when subsurface sediments are within the gas hydrate stability zone, the gas solubility in pore water will decrease from the deep to the shallow (Rempel and Buffett, 1997; Zatsepina and Buffett, 1997, 1998; Yang et al., 2001; Servio and Englezos, 2002; Davie et al., 2004). If methane concentrations are constantly provided from the deep, the gas hydrate fraction is more and more accumulated in the shallow. It can be clearly seen from the empirical expressions (Fig. 7). It is consistent with the fact that in the Hydrate Ridge area the largest concentration of gas hydrate exists in the shallower part of the gas hydrate occurrence zone while it is less concentrated in the deeper part (Expedition 311 Scientists, 2005). If the gas hydrate fraction in the Hydrate Ridge area is quantitatively calculated with the empirical expression (Fig. 8), it can be comparable with that speculated from the geophysical logging data (Lee et al., 2006; Fig. 9).

Of course, in reality especially in local environments the situation is complicated. For example, in subsurface sediments, if methane cannot be provided continuously and sufficiently from the deep to the shallow, gas hydrate will possibly preferably occur just nearby the locations where methane is supplied. In the Blake Ridge area, gases are supplied by the biogenic process, hence gas hydrates are accumulated just close to the BSR within the gas hydrate stability zone (Paull and Matsumoto, 2000).

For the empirical expression predicting gas hydrate density, although there are either no experimental data available to confirm, it is still clear that the gas hydrate density decreases with the gas hydrate equilibrium pressure and the gas hydrate mass-density increases with the ethane percentage in the gas mixture (Fig. 10).

Conclusions

A general agreement between the correlated expressions and the experimental data and other models shows the reliability of the empirical expressions for predicting gas hydrate stability in different systems within the given appropriate parameter ranges. The deflection of the empirical predictions for gas hydrate stability from the experimental data indicates the constraint of the originally based van der Waals model at high temperatures (>290.15K).

Other empirical expressions for predicting gas hydrate stability in other systems and evaluating gas hydrate fraction out of pore space and gas hydrate density need further validations due to lack of available experimental data at the moment. However, the predicted results show that effects of pore size and salinity on gas hydrate fraction are negligible and that gas hydrate density is nearly independent of pore sizes and salinities.

The empirical expression for gas hydrate fraction shows that the methane concentration plays an important role in controlling gas hydrate fraction. Gas hydrate fraction may rise greatly with the increase of methane concentration and it could obviously decrease with the increase of pressure at a constant gas concentration within the gas hydrate stability zone.

From the empirical expression of gas hydrate density changing with ethane percentage with respect to methane, it is extracted that the density tends to decrease with the increase of pressure and increase with the ethane percentage in the gas mixture.

Acknowledgements

We thank Drs. R. Thiéry and D. Dalmazzone for their constructive suggestions. This work is supported by French-Chinese Foundation of Science and Its Application (FFCSA) and by China Scholarship Council (CSC). It is also financed by China's project "study of modeling technology on gas hydrate formation conditions over the permafrost in the Qinghai-Tibet plateau" (K2007-2-5). One of the authors, LU Zhengquan, thanks professor Jacques Caen and Madame Anne-Sophie Caen for their sincere support.

References

- Anderson, R., M. Llamedo, B. Tohidi, R. W. Burgass, 2003. Experimental measurement of methane and carbon dioxide clathrate hydrate equilibria in mesoporous silica. *J. Phys. Chem. B* 2003, 107, 3507-3514.
- Bakker, R.J., J. Dubessy, M. Cathelineau, 1996. Improvements in clathrate modelling: I. The H₂O-CO₂ system with various salts. *Geochimica et Cosmochimica Acta*, Vol. 60, No. 10, pp1657-1681.
- Charlou, J.L., J.P. Donval, Y. Fouquet, H. Ondreas, J. Knoery, P. Cochonat, D. Levaché, Y. Poirier, P. Jean-Baptiste, E. Fourré, B. Chazallon, the ZAIROV Leg 2 Scientific Party, 2004. Physical and chemical characterization of gas hydrates and associated methane plumes in the Congo-Angola Basin. *Chemical Geology*, 205 (2004), 405-425.
- Cisternas, L.A., E.J. Lam, 1991. An analytic correlation for the vapour pressure of aqueous and non-aqueous solutions of single and mixed electrolytes part II: application and extension. *Fluid Phase Equilib.*, 62, 11-27.

- Clennell, M.B., M. Hovland, J.S. Booth, P. Henry, W.J. Winter, 1999. Formation of natural gas hydrates in marine sediments 1: conceptual model of gas hydrate growth conditioned by host sediment properties. *J. Geophys. Res. B*, 104, 22985-23003.
- Davie, M. K., B.A. Buffett, 2001. A numerical model for the formation of gas hydrate below the seafloor. *Journal of Geophysical Research*, Vol.106, No.B1, 497-514.
- Davie, M.K., O.Y. Zatsepina, B.A. Buffett, 2004. Methane solubility in marine hydrate environments. *Marine Geology*, 203 (2004), 177-184.
- Deaton, W.M., Frost, E.M., Jr., 1946. Gas hydrates and their relation to the operation of natural-gas pipe lines. U.S. Bureau of Mines Monograph, 8, Department of the Interior, 10.
- Dholabhai, P. D. and P. R. Bishnoi, 1994. Hydrate equilibrium conditions in aqueous electrolyte solutions: mixtures of methane and carbon dioxide. *J. Chem. Eng. Data*, Vol.39, No.1, 191-194.
- Dholabhai, P.D., J.S. Parent, P.R. Bishnoi, 1997. Equilibrium conditions for hydrate formation from binary mixtures of methane and carbon dioxide in the presence of electrolytes, methanol and ethylene glycol. *Fluid Phase Equilibria*, Vol.141, No.1, 235-246.
- Dickens, G.R., 2001. Modeling the global carbon cycle with a gas hydrate capacitor: significance for the latest Paleocene thermal maximum. In: Paull, C.K., W.P. Dillon, (Eds.), *Natural gas hydrates: occurrence, distribution and detection*, Geophysical Monograph Series, 124, American Geophysical Union, 19-40.
- Dickens, G. R. and M. S. Quinby-Hunt, 1994. Methane hydrate stability in seawater. *Geophysical Research Letters*, Vol.21, No.19, 2115-2118.
- Dickens, G. R. and M. S. Quinby-Hunt, 1997. Methane hydrate stability in pore water: A simple theoretical approach for geophysical applications, *Journal of Geophysical Research*, 102, pp773-783.
- Dillon, W.P., Nealon, J.W., Taylor, M.H., Lee, M.W., Drury, R.M., Anton, C.H., 2001. Seafloor collapse and methane venting associated with gas hydrate on the Blake Ridge—causes and implications to seafloor stability and methane release. In: Paull, C.K., W.P. Dillon, (Eds.), *Natural gas hydrates: occurrence, distribution and detection*, Geophysical Monograph, 124, American Geophysical Union, 211-233.
- Elgibaly, A. A., A. M. Elkamel, 1998. A new correlation for predicting hydrate formation conditions for various gas mixtures and inhibitors. *Fluid Phase Equilibria*, Vol. 152, No. 1, 23-42.
- Expedition 311 Scientists, 2005. Cascadia margin gas hydrates. *IODP Prel. Rept.*, 311. doi:10.2204/iodp.pr.311.2005.
- Gayet, P., C. Dicharry, G. Marion, A. Graciaa, J. Lachaise, A. Nesterov, 2005. Experimental determination of methane hydrate dissociation curve up to 55MPa by using a small amount of surfactant as hydrate promoter. *Chemical Engineering Science*, 60 (2005), 5751–5758.
- Glew, D. N., 2003. Aqueous nonelectrolyte solutions — part XX: formula of structure I methane hydrate, congruent dissociation melting point, and formula of the metastable hydrate. *Can. J. Chem.* Vol.81, 1443-1450.
- Griffiths, F.J. and R.C. Joshi, 1989. Change in pore size distribution due to consolidation of clays. *Geotechnique*, 39, 159-167.
- Hammerschmidt, E.G., 1934. Formation of gas hydrates in natural gas transmission lines. *Ind. Eng. Chem.*, 26, 851-855.
- Handa, Y. P. and D. Stupin, 1992. Thermodynamic properties and dissociation characteristics of methane and propane hydrates in 70Å radius silica gel pores. *J. Phys. Chem.* Vol.96, No.21, 8599-8603.
- Handa, Y. P., 1990. Effect of hydrostatic pressure and salinity on the stability of gas hydrates. *J. Phys. Chem.* 1990, 94, 2652-2657.
- Henry, P., M. Thomas, M.B Clennell, 1999. Formation of natural gas hydrates in marine sediments 2: thermodynamic calculations of stability conditions in porous sediments. *J. Geophys. Res.*, Vol.104, No.B10, 23005-23022.
- Jager, M.D., E.D. Sloan, 2001. The effect of pressure on methane hydration in pure water and sodium chloride solutions. *Fluid Phase Equilibria*, 185 (2001), 89–99.
- Klauda, J. B., S. I. Sandler, 2003. Predictions of gas hydrate phase equilibria and amounts in natural sediment porous media. *Marine and Petroleum Geology*, 20 (2003), 459-470.
- Kvenvolden, K.A., 2002. Methane hydrate in the global organic carbon cycle. *Terra Nova*, 14, 302-306.
- Kvenvolden, K. A., 1995. A review of the geochemistry of methane in natural gas hydrate. *Org. Geochem.* Vol. 23, No. 11/12, 997-1008.
- Lee, M.W., T.S. Collett, 2006. Gas hydrate and free gas saturations estimated from velocity logs on Hydrate Ridge, offshore Oregon, USA. In Tréhu, A.M., Bohrmann, G., Torres, M.E., and Colwell, F.S. (Eds.) *Proceedings of the Ocean Drilling Program, Scientific Results* Volume 204.

Lorenson, T.D., Collett, T.S., 2000. Gas content and composition of gas hydrate from sediments of the southeastern North American continental margin. In: Paul, C.K., Matsumoto, R., Wallace, P.J., Dillon, W.P. (Eds.), *Proceedings of the Ocean Drilling Program, Scientific Results 164*, Ocean Drilling Program, College Station, Texas, 37-46.

Lu, H., R. Matsumoto, 2005. Experimental studies on the possible influences of composition changes of pore water on the stability conditions of methane hydrate in marine sediments. *Marine Chemistry*, 93 (2005), 149-157.

Maekawa, T., 2001. Equilibrium conditions for gas hydrates of methane and ethane mixtures in pure water and sodium chloride solution. *Geochemical Journal*, vol.35, 59-66.

Maslin, M., C. Vilela, N. Mikkelsen, P. Grootes, 2005. Causes of catastrophic sediment failures of the Amazon Fan. *Quaternary Science Reviews*, 24 (2005), 2180–2193.

Masoudi, R. and B. Tohidi, 2005. Estimating the hydrate stability zone in the presence of salts and/or organic inhibitors using water partial pressure. *Journal of Petroleum Science and Engineering*, 46 (2005), 23-36.

Milkov, A. V., 2004. Global estimates of hydrate-bound gas in marine sediments: how much is really out there? *Earth-Science Reviews*, 66 (2004), 183-197.

Østergaard, K.K., A. Danesh, B. Tohidi, A.C. Todd, R.W. Burgass, 2000. A general correlation for predicting the hydrate free zone of reservoir fluids. *SPE Prod. Facil.*, 15 (4), 228-233.

Østergaard, K. K., R. Masoudi, B. Tohidi, A. Danesh, A. C. Todd, 2005. A general correlation for predicting the suppression of hydrate dissociation temperature in the presence of thermodynamic inhibitors. *Journal of Petroleum Science and Engineering*, 48 (2005), 70-80.

Paull, C. K., R. Matsumoto, 2000. Leg 164 overview. In Paull, C.K., R. Matsumoto, P.J. Wallace, W.P. Dillon, (Eds.), 2000. *Proc. ODP, Sci. Results*, 164: College Station, TX (Ocean Drilling Program).

Rempel, A.W., Buffett, B.A., 1997. Formation and accumulation of gas hydrate in porous media. *J. Geophys. Res.* 102 (B5), 10151-10164.

Rempel, A.W., B.A. Buffett, 1998. Mathematical models of gas hydrate accumulations. In: Henriot, J.P., Mienert, J. (Eds.), *Gas hydrates: relevance to world margin stability and climatic change*, Geol. Soc. London Spec. Publ., 137, 63-74.

Seo, Y. T. and H. Lee, 2001. Multi-phase hydrate equilibria of the ternary carbon dioxide, methane, and water mixtures. *J. Phys. Chem. B* 2001, 105, 10084-10090.

Servio, P., F. Lagers, C. Peters, P. Englezos, 1999. Gas hydrate phase equilibrium in the system methane–carbon dioxide–neohexane and water. *Fluid Phase Equilibria*, 158-160 (1999), 795-800.

Servio, P., P. Englezos, 2002. Measurement of dissolved methane in water in equilibrium with its hydrate. *J. Chem. Eng. Data*, 47, 87-90.

Shipboard Scientific Party, 2003. Leg 204 summary. In Tréhu, A.M, Bohrmann, G., Rack, F.R., Torres, M.E., et al., *Proc. ODP, Init. Repts.*, 204: College Station TX (Ocean Drilling Program), 1-75.

Sloan Jr., E.D., 1998. *Clathrate hydrates of natural gases*. 2nd edition. Marcel Dekker, New York.

Subramanian, S., R.A. Kini, S.F. Dec, E.D. Sloan Jr, 2000. Evidence of structure II hydrate formation from methane + ethane mixtures. *Chemical Engineering Science*, 55 (2000), 1981-1999.

Sultan, N., J.P. Foucher, P. Cochonat, T. Tonnerre, J.F. Bourillet, H. Ondreas, E. Cauquil, D. Grauls, 2004b. Dynamics of gas hydrate: case of the Congo continental slope. *Marine Geology*, 206 (2004), 1-18.

Sultan, N., P. Cochonat, J.P. Foucher, J. Mienert, 2004c. Effect of gas hydrates melting on seafloor slope instability. *Marine Geology*, 213 (2004), 379-401.

Sultan, N., P. Cochonat, M. Canals, A. Cattaneo, B. Dennielou, H. Hafidason, J.S. Laberg, D. Long, J. Mienert, F. Trincardi, R. Urgeles, T.O. Vorren, C. Wilson, 2004a. Triggering mechanisms of slope instability processes and sediment failures on continental margins: a geotechnical approach. *Marine Geology*, 213 (2004), 291-321.

Takeya, S., M. Kida, H. Minami, H. Sakagami, A. Hachikubo, N. Takahashi, H. Shoji, V. Soloviev, K. Wallmann, N. Biebow, A. Obzhairov, A. Salomatin, J. Poort, 2006. Structure and thermal expansion of natural gas clathrate hydrates. *Chemical Engineering Science*, 61 (2006), 2670-2674.

Tishchenko, P., C. Hensen, K. Wallmann, C. S. Wong, 2005. Calculation of the stability and solubility of methane hydrate in seawater. *Chemical Engineering*, 219 (2005), 37-52.

Turner, D. J., R. S. Cherry, E. D. Sloan, 2005. Sensitivity of methane hydrate phase equilibria to sediment pore size. *Fluid Phase Equilibria*, 228-229 (2005), 505-510.

Uchida, T., T. Ebinuma, S. Takeya, J. Nagao, H. Narita, 2002. Effects of pore sizes on dissociation temperatures and pressures of methane, carbon dioxide, and propane hydrates in porous media. *J. Phys. Chem. B* 2002, 106, 820-826.

Uchida, T., T. Ebinuma, T. Ishizaki, 1999. Dissociation condition measurements of methane hydrate in confined small pores of porous glass. *J. Phys. Chem. B* 1999, 103, :3659-3662.

Van der Waals, J.A., J.C. Platteeuw, 1959. Clathrate Solutions. *Adv. Chem. Phys.* 2, 2-57.

Xu, W., C. Ruppel, 1999. Predicting the occurrence, distribution, and evolution of methane gas hydrate in porous marine sediments. *Journal of Geophysical Research*, Vol.104, No.B3, 5081-5095.

Yang, S.O., S.H. Cho, H. Lee, C.S. Lee, 2001. Measurement and prediction of phase equilibria for water + methane in hydrate forming conditions. *Fluid Phase Equilibria*, 185 (2001), 53–63.

Zatsepina, O.Y., B.A. Buffet, 1998. Thermodynamic conditions for the stability of gas hydrate in the seafloor. *Journal of Geophysical Research*, Vol.103, No.B10, 24127-24139.

Zatsepina, O. Y., B. A. Buffet, 1997. Phase equilibrium of gas hydrate: implications for the formation of hydrate in the deep sea floor. *Geophysical Research Letters*, Vol.24, No.13, 1567-1570.

Zhang, Y., P. G. Debeneditti, R. K. Prud'homme, B. A. Pethica, 2005. Accurate prediction of clathrate hydrate phase equilibria below 300K from a simple model. *Journal of Petroleum Science and Engineering*, 51 (2005), 42-53.

Tables

Table 1 List of the designed systems in correlation of gas hydrate formation

System No.	CH ₄	C ₂ H ₆	H ₂ S	CO ₂	pure water	pore water	pore size	seawater
01	●				●			
02	●	●			●			
03	●		●		●			
04	●			●	●			
05	●					●		
06	●						●	
07	●						●	●
08	●	●				●		
09	●		●			●		
10	●			●		●		

Note: ●--signifies consideration of various factors affecting gas hydrate formation system

Table 2 Relevant variables and parameters in correlated equations for gas hydrate equilibrium

Systems	Equations	Variable ranges	Parameters	Rs-squared, points
CH ₄ +H ₂ O	Eq. (4)	T: 273.15-290.15K P: 1500-40000kPa	A: 0.1045998173 B: 1.01337211×10 ⁻⁹	0.998792, 482
CH ₄ +C ₂ H ₆ + H ₂ O	Eq. (5)	Me: 0 (exclusive) -10	Ce: 0.001743551779 De: 0.1053746708	0.989815, 8
			Ee: -0.5458198173 Fe: 0.8031850629×10 ⁻⁹	0.990577, 8
CH ₄ +H ₂ S+ H ₂ O	Eq. (6)	Mh: 0 (exclusive) -8	Ch: 0.003073015158 Dh: 0.1066400891	0.984682, 13
			EH: -1.014974813 Fh: 0.5464837042×10 ⁻⁹	0.986926, 13
CH ₄ +CO ₂ + H ₂ O	Eq. (7)	Mc: 0 (exclusive) -20	Cc: 0.0004290004837 Dc: 0.1045713821	0.999236, 18
			Ec: -0.135446772 Fc: 1.016136845×10 ⁻⁹	0.999533, 18
CH ₄ + NaCl + H ₂ O	Eq. (8)	S: 0 (exclusive) -0.050 mol NaCl per mol H ₂ O	Cs: 0.1711726397 Ds: 0.1046133676	0.999805, 22
			Es: -34.14836102 Fs: 1.010769956×10 ⁻⁹	0.999625, 22
CH ₄ + H ₂ O + Pore size	Eq. (9)	R: 6×10 ⁻⁹ -1×10 ⁻⁶ meter of pore radius	Ra: 2.830542962×10 ⁻¹¹ Rb: 0.104638146	0.998598, 13
			Rc: -3.312874659×10 ⁻¹⁸ Rd: 9.8640645×10 ⁻¹⁰	0.997453, 13
CH ₄ + Seawater + Pore size	Eq. (9)	R: 6×10 ⁻⁹ -1×10 ⁻⁶ meter of pore radius	Ra: 3.053808015×10 ⁻¹¹ Rb: 0.1065001844	0.999441, 13
			Rc: -2.490775613×10 ⁻¹⁸ Rd: 0.6834013617×10 ⁻⁹	0.992911, 13
CH ₄ +C ₂ H ₆ + NaCl + H ₂ O	Eq. (10)	Me: 0 (exclusive) -5 S: 0-0.08014 mol NaCl out of pore water	Ce ₁ : 0.01065187252 Ce ₂ : 0.002021155646	0.998051, 6
			De ₁ : 0.1758750175 De ₂ : 0.1048323571	0.999801, 6
			Ee ₁ : -2.794741198 Ee ₂ : -0.6303566695	0.998105, 6
			Fe ₁ : -34.92161276 Fe ₂ : 0.9372047997×10 ⁻⁹	0.99987, 6
CH ₄ +H ₂ S+ NaCl + H ₂ O	Eq. (11)	Mh: 0 (exclusive) -3 S: 0-0.05994 mol NaCl out of pore water	Ch ₁ : 0.03146516458 Ch ₂ : 0.004011976207	0.991668, 5
			Dh ₁ : 0.1763278999 Dh ₂ : 0.1050973	0.999863, 5
			EH ₁ : -8.635077998 EH ₂ : -1.30225971	0.991865, 5
			Fh ₁ : -35.32491058 Fh ₂ : 0.8713968411×10 ⁻⁹	0.999854, 5
CH ₄ +CO ₂ + NaCl + H ₂ O	Eq. (12)	Mc: 0 (exclusive) -3 S: 0-0.05994 mol NaCl out of pore water	Cc ₁ : 0.000419793886 Cc ₂ : 0.0009341330952 Cc ₃ : 0.03464474167	0.997332 (second degree), 5
			Dc ₁ : 0.1739887194 Dc ₂ : 0.1045756253	0.999781, 5

			$EC_1: -1.103423658 \times 10^{-10}$ $EC_2: 2.978552143 \times 10^{-9}$ $EC_3: -2.410085873 \times 10^{-8}$	0.996242 (second degree), 5
			$FC_1: -34.87559599$ $FC_2: 1.009068322 \times 10^{-9}$	0.99971, 5

Table 3 AADPs between the predicted results and the experimental data

hydrate formation system	ADPs* range (%)	AADPs** (%)	data source
CH ₄ + H ₂ O	0.04-3.57	2.08	Dickens et al., 1994 (7)
	0.01-3.82	1.49	Maekawa 2001 (30)
	0.74-6.95	2.24	Yang et al., 2001 (10)
	0.04-6.75	1.47	Gayet et al., 2005 (16)
	0.09-4.45	1.52	Glew, 2003 (23)
97.9mol% CH ₄ + 2.1mol% C ₂ H ₆ + H ₂ O	0.23-2.14	1.23	Maekawa, 2001 (10)
98.9mol% CH ₄ + 1.1mol% C ₂ H ₆ + H ₂ O	0.27-6.22	2.74	Maekawa, 2001 (13)
95.2mol% CH ₄ + 4.8mol% C ₂ H ₆ + H ₂ O	1.78-11.58	7.18	Maekawa, 2001 (14)
CH ₄ + 3.0wt% NaCl out of H ₂ O	2.42-5.86	3.61	Maekawa, 2001 (7)
CH ₄ + 3.35wt% NaCl out of H ₂ O	1.99-10.90	4.91	Dickens et al., 1994 (10)
CH ₄ + 0.02001mol% NaCl out of H ₂ O	2.39-13.68	8.47	Jager et al., 2001 (3)
97.9mol% CH ₄ + 2.1mol% C ₂ H ₆ + 3.0wt% NaCl out of H ₂ O	3.93-7.28	5.68	Maekawa, 2001 (8)
95.2mol% CH ₄ + 4.8mol% C ₂ H ₆ + 3.0wt% NaCl out of H ₂ O	9.28-13.88	11.56	Maekawa, 2001 (8)
80mol% CH ₄ + 20mol% CO ₂ + H ₂ O	9.72-15.45	12.36	Dholabhai et al., 1994, 1997 (6)
	5.08-14.0	8.14	Servio et al., 1999 (5)
	7.22-11.88	10.53	Seo et al., 2001 (3)
CH ₄ + H ₂ O + 6.0nm pore size	20.70-24.96	22.83	Uchida et al., 2002 (2)
CH ₄ + H ₂ O + 7.0nm pore size	3.83-8.52	6.20	Handa et al., 1992 (3)
CH ₄ + H ₂ O + 9.2nm pore size	10.52-12.24	11.57	Anderson et al., 2003 (3)
CH ₄ + H ₂ O + 10.0nm pore size	9.53-15.04	12.54	Uchida et al., 1999, 2002 (3)
CH ₄ + H ₂ O + 15.8nm pore size	2.62-7.29	4.35	Anderson et al., 2003 (4)
CH ₄ + H ₂ O + 30.0nm pore size	0.40-7.98	2.68	Uchida et al., 1999, 2002 (13)
CH ₄ + H ₂ O + 30.6nm pore size	0.76-5.37	2.64	Anderson et al., 2003 (3)
CH ₄ + H ₂ O + 50.0nm pore size	1.22-3.83	2.08	Uchida et al., 1999, 2002 (4)
CH ₄ + H ₂ O + 100.nm pore size	0.88-6.19	2.64	Uchida et al., 1999, 2002 (6)

Note: *--the absolute deviation of pressures for each pair point (ADPs = $\text{abs}(P_{\text{experiment}} - P_{\text{prediction}}) / P_{\text{experiment}}$); **--the average absolute deviation of pressures for all the pair points of one group set (AADPs = $\text{average}(\text{abs}(P_{\text{experiment}} - P_{\text{prediction}}) / P_{\text{experiment}})$).

Table 4 Relevant variables and parameters in correlated equations for gas hydrate fraction and its density

Systems	Equations	Variable ranges	Parameters	Rs-squared, points
CH ₄ +H ₂ O	Eq. (13)	T: 273.15-290.15K P: 1500-40000kPa M: 4×10 ⁻³ - 0.15 mol/mol H ₂ O	<i>Fa</i> ₁ : 3.372819758 <i>Fa</i> ₂ : -0.0146473394 <i>Fa</i> ₃ : -3.342336281 <i>Fa</i> ₄ : -0.004074376116	0.993491, 16
			<i>Fb</i> ₁ : -0.2926569378 <i>Fb</i> ₂ : -30 <i>Fb</i> ₃ : 1.197540315 <i>Fb</i> ₄ : 0.08689668992	0.99984, 16
CH ₄ +C ₂ H ₆ + H ₂ O	Eq. (14)	T: 273.15-290.15K P: 1500-40000kPa Me: 0 (exclusive) - 3	<i>Da</i> ₁ : 0.5996244768 <i>Da</i> ₂ : 0.03264272614 <i>Da</i> ₃ : -0.00497352021	0.991983, 5
			<i>Db</i> ₁ : 6.300233839×10 ⁻⁸ <i>Db</i> ₂ : 4.523123336×10 ⁻⁸	0.990242, 4
			<i>Dc</i> ₁ : 0.02773021069 <i>Dc</i> ₂ : 0.2915045823	0.987395, 5
			<i>Dd</i> ₁ : 0.009992175158 <i>Dd</i> ₂ : -0.01488030989 <i>Dd</i> ₃ : 0.002216034151	0.99148, 5

Figures

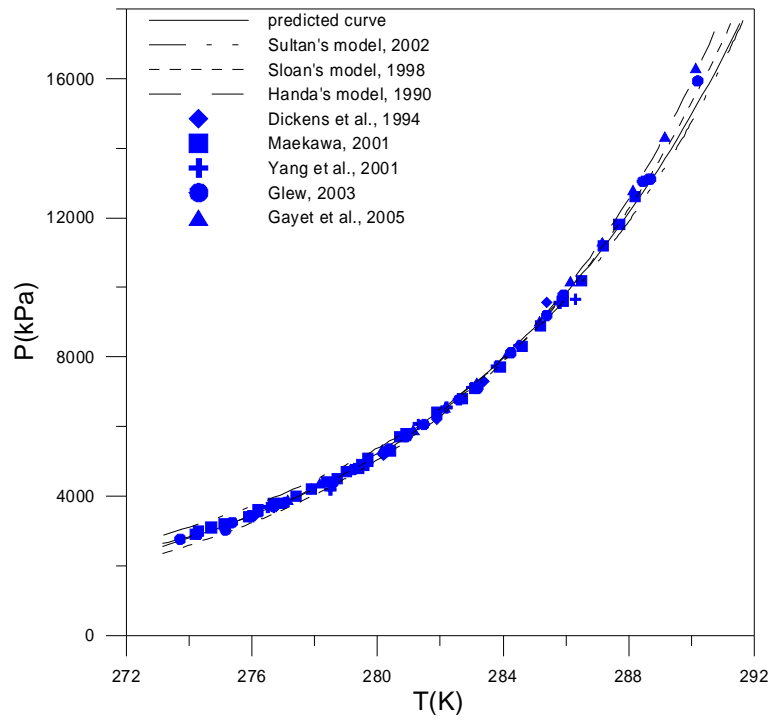


Fig. 1 Comparison between the predicted results and the experimental data as well as the predecessors' modelled results based on pure methane and pure water system

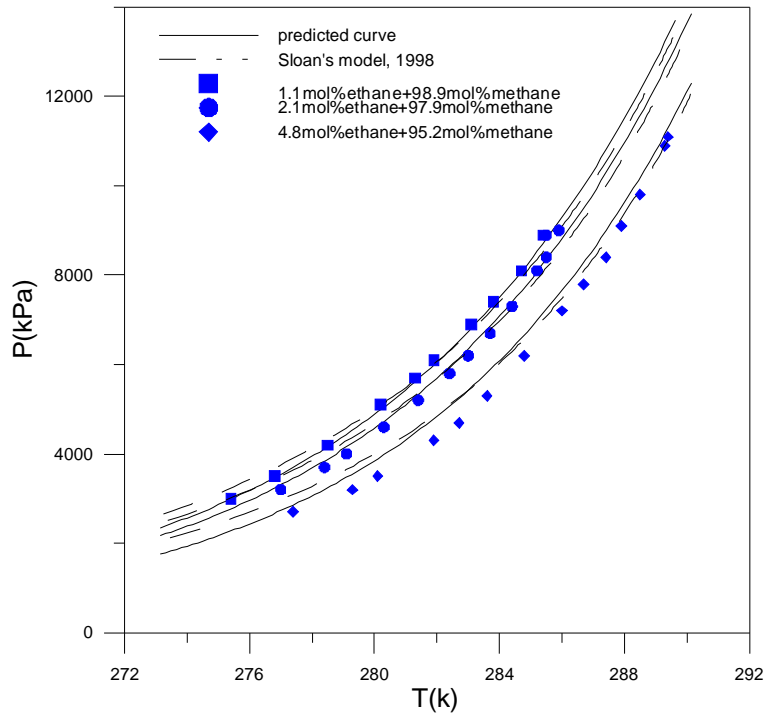


Fig. 2 Comparison between the predicted results and the experimental data (Maekawa, 2001) from the mixture of methane and ethane in pure water system

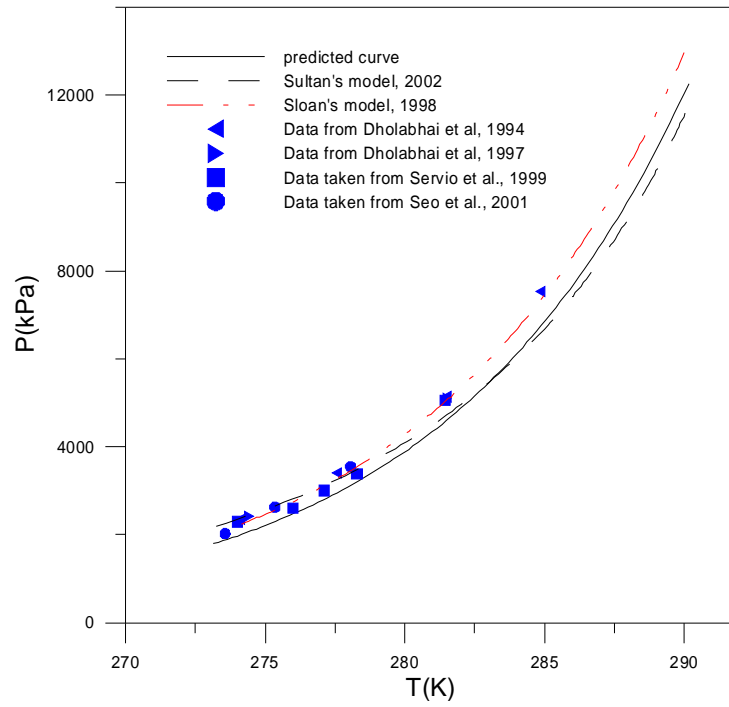


Fig. 3 Comparison between the predicted results and the experimental data from the mixture of 80 mol% methane and 20 mol% carbon dioxide in pure water system

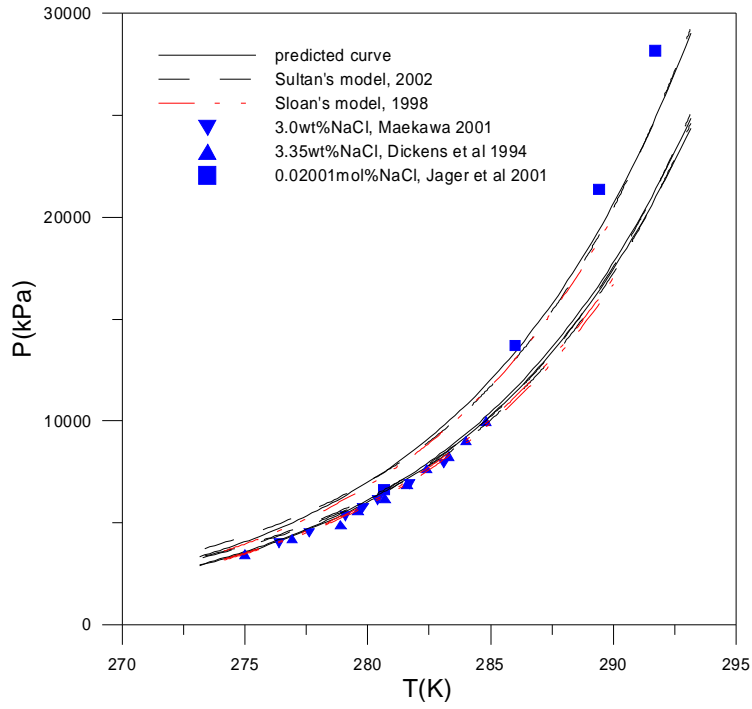


Fig. 4 Comparison between the predicted results and the experimental data in pure methane and pore water system

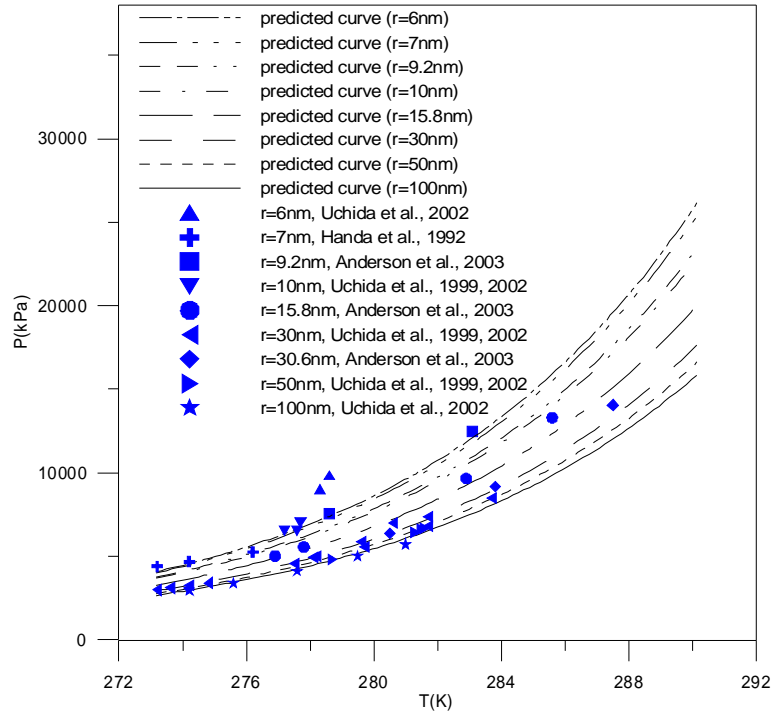


Fig.5 Comparison between the predicted results and the experimental data from pure methane and pure water system in porous media

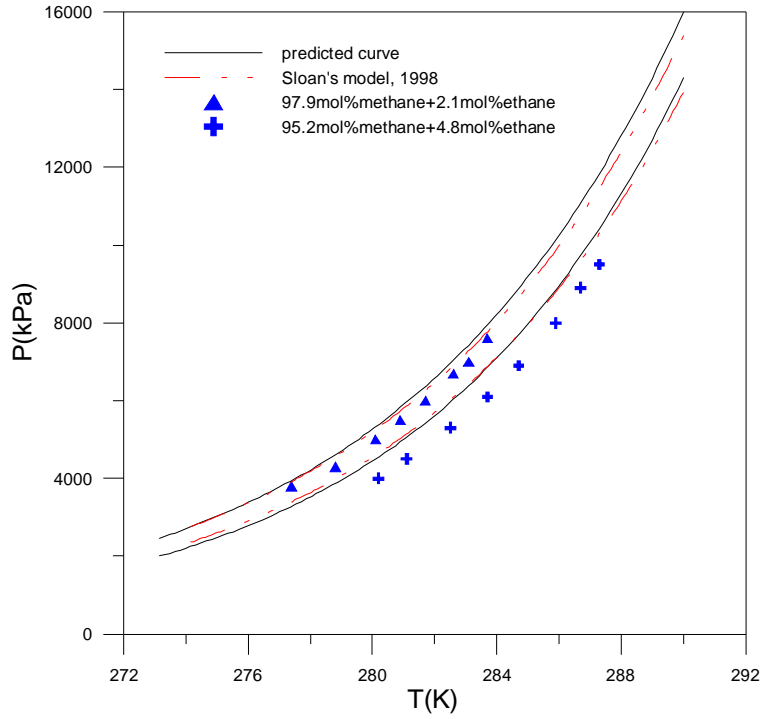


Fig. 6 Comparison between the predicted results and the experimental data (Maekawa, 2001) for the mixture of methane and ethane in 3.0wt% NaCl system

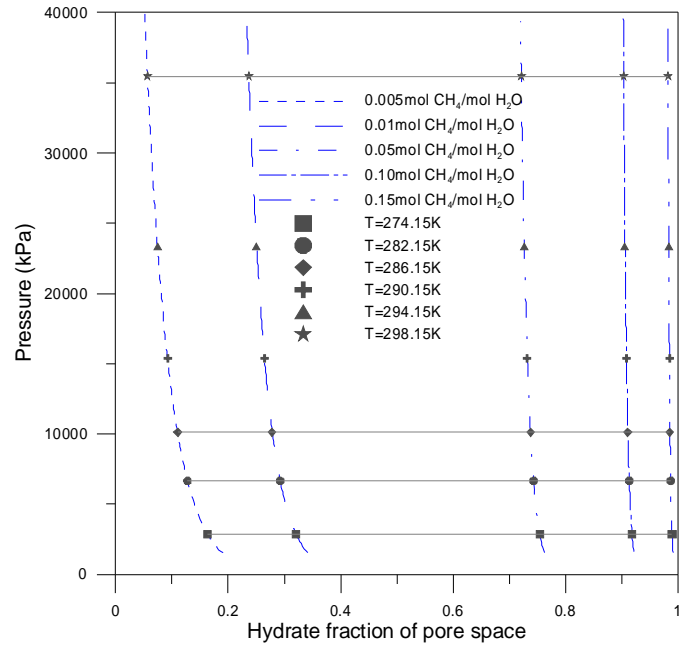


Figure 7 Gas hydrate fraction as a function of pressure and bulk methane concentrations

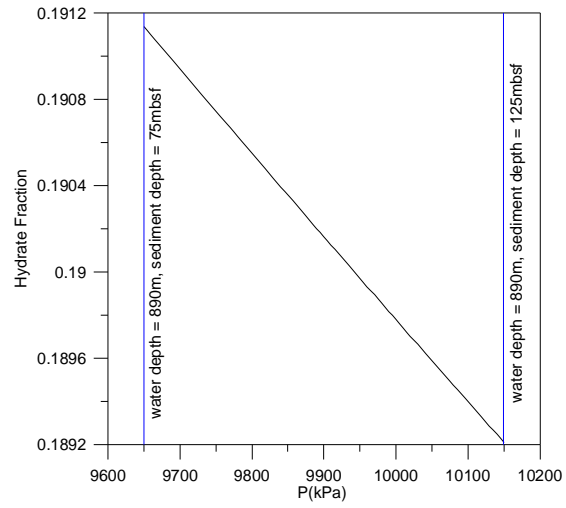


Fig. 8 Prediction for gas hydrate fraction at site 1244 of Hydrate Ridge
 Note: water depth is 890m, assuming that methane concentration in sediment is 0.007 mol/mol water and hydrostatic pressure is equal to 100kPa/10m.

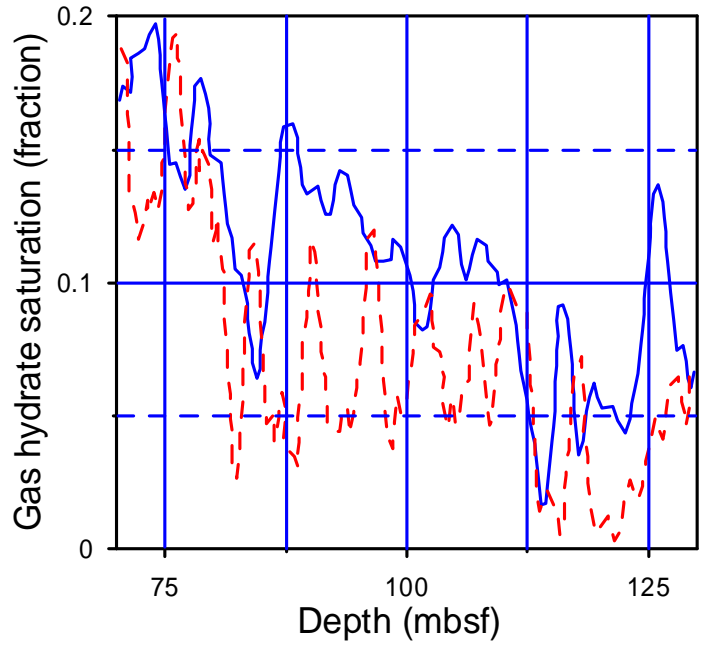


Fig. 9 Gas hydrate saturations estimated from the S-wave velocity (solid) and the electrical resistivity log (dash) at site 1244 of Hydrate Ridge (Lee et al., 2006)

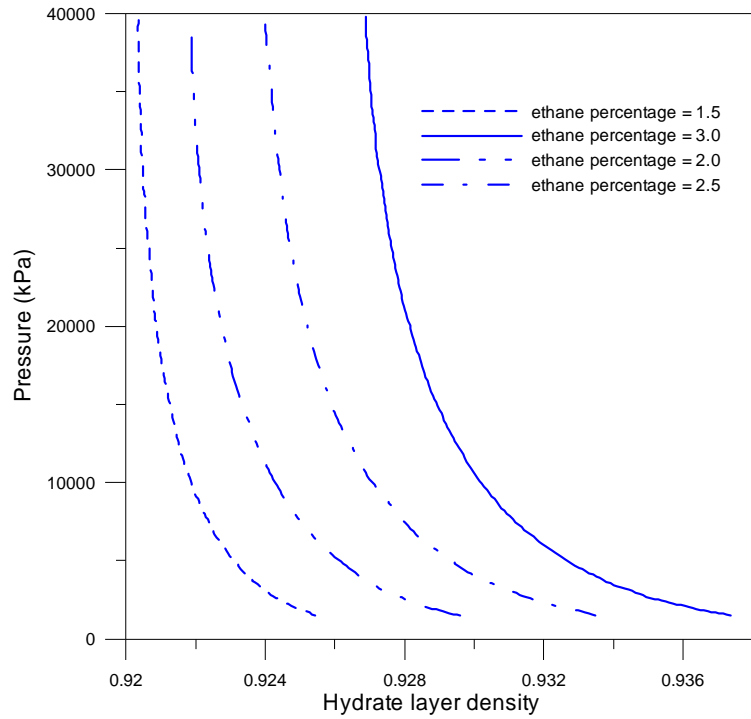


Fig. 10 Schematic relations of gas hydrate density to pressure at different ethane percentage with respect to methane